ChemComm

COMMUNICATION

View Article Online
View Journal | View Issue

Check for updates

Cite this: *Chem. Commun.*, 2025, **61**, 576

Received 3rd August 2024,
Accepted 29th November 2024

DOI: 10.1039/d4cc03956d

rsc.li/chemcomm

Multicomponent synthesis of stereogenic-at-boron fluorophores (BOSPYR) from boronic acids, salicylaldehydes, and 2-formylpyrrole hydrazones†

Ezgi Bayer Kömüşdoğan, [a] Sania Batool, [a] Ertan Şahin, [b] Erol Yildirim, [a] Murat Işık *[c] and Cihangir Tanyeli *[a]

This work describes one-step syntheses of various stereogenic-at-boron fluorochromes (BOSPYR) *via* multicomponent reactions involving readily accessible boronic acids, salicylaldehydes, and 2-formylpyrrole hydrazones. The dyes absorb and emit in the visible region of the electromagnetic radiation, and are characterized by large Stokes shifts (2850–4930 cm^{-1}) with weak fluorescence emissions (Φ_{fl}: 1.5–9.1%). Notably, the dimmed fluorescence of BOSPYRs recovers upon transition to viscous media (21-fold for 1a). The representative compound 1a exhibits clear Cotton effects with dissymmetry factors of *ca.* $|g_{abs}| \sim 1.9 \times 10^{-3}$ in the visible region, indicating efficient asymmetry induction to the chromophore. The X-ray molecular structure of 1a shows that the chromophore deviates from planarity by 17.2°, which may contribute significantly to the inherent chirality of the fluorophore. A computational examination of excited states by time-dependent density functional theory (TD-DFT) identifies the emission mechanism as arising from a locally-excited (LE) state.

Fluorophores have become indispensable tools across various disciplines, including chemistry, biology, medicine, materials science, and numerous interdisciplinary areas.[1] The element boron (B) plays a crucial role in modern fluorophore design thanks to forming stable tetravalent chelates, thereby restricting internal bond rotations in the π-skeleton of nascent fluorophores, enforcing planarity, and ensuring enhanced π-conjugation throughout the dye.[2] This can be well exemplified by the archetypal boron dipyrromethene (BODIPY, Fig. 1) dyes[3] or similar heterocyclic architectures, locked typically with a difluoro boron bridge.[2] Despite their successful application as functional dyes in diverse fields, from probes/labels to photosensitizers for photodynamic action, the synthesis of such functional BODIPYs often involves intricate, long linear routes.[4]

Unlike conventional synthesis approaches, multicomponent reactions (MCRs) offer a convergent synthesis approach, assembling often readily available starting materials in a single step. This has recently sparked growing interest in the development of functional organic dyes through MCRs.[5,6] In contrast to the commonly used BF_3, the group of Gois & Pischel has employed arylboronic acids as the boron source for the MCR-based development of intriguing BASHY fluorophores (Fig. 1),[6] which exhibit photophysical properties highly comparable to BODIPYs.[6–12] Notably, the sp^3 hybridized boron atom in these dyes, accommodating four distinct ligands, creates asymmetry around it, imparting chirality to the dye.[9]

This remains a challenge in BODIPYs due to their highly symmetric nature (point group: C_{2v}),[13–15] particularly for those with chiral-at-boron arrangements.[15] Therefore, currently, the majority of chiral-at-boron chromophores/fluorophores, although rare in number, generally rely on other miscellaneous heterocyclic systems with a tetravalent boron center.[16] The visible light-absorbing BASHY fluorophores, as solely stereogenic-at-boron dyes, exhibited detectable chiroptical activities in electronic circular dichroism (ECD) and circularly polarized luminescence (CPL) spectroscopy within the visible region.[9] Similarly, although not a true MCR-type synthesis, research efforts by Hao & Jiao and co-workers employing arylboronic acids as the locking unit have

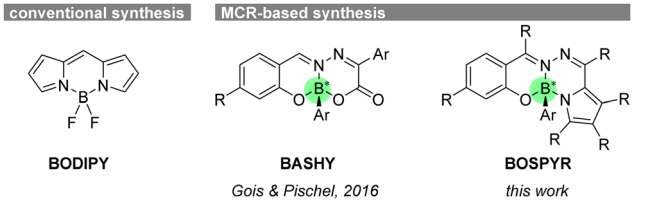

Fig. 1 BODIPY dyes accessible through conventional synthesis *vs.* BASHY dyes and BOSPYR dyes (this work) through MCR approach.

[a] *Department of Chemistry, Middle East Technical University, 06800 Ankara, Turkey. E-mail: tanyeli@metu.edu.tr*
[b] *Department of Chemistry, Atatürk University, Erzurum, 25240, Turkey*
[c] *Department of Food Engineering, Bingöl University, Bingöl, 12000, Turkey. E-mail: misik@bingol.edu.tr*

† Electronic supplementary information (ESI) available: Experimental and crystallographic details. CCDC 2344453. For ESI and crystallographic data in CIF or other electronic format see DOI: https://doi.org/10.1039/d4cc03956d

Open Access Article. Published on 05 N'wendzamhala 2024. Downloaded on 2026-05-24 15:17:00.
This article is licensed under a Creative Commons Attribution-NonCommercial 3.0 Unported Licence.

This journal is © The Royal Society of Chemistry 2025

Open Access Article. Published on 05 N'wendzamhala 2024. Downloaded on 2026-05-24 15:17:00.
This article is licensed under a Creative Commons Attribution-NonCommercial 3.0 Unported Licence.

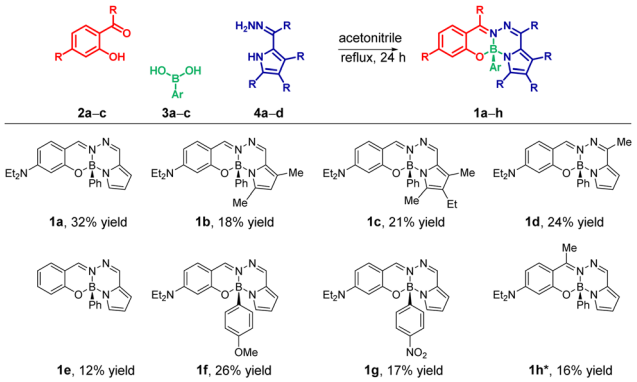

Scheme 1 Tri-component modular synthesis of BOSPYR dyes (**1a–h**): substrate scope. *The synthesis of compound **1h** was achieved by employing the hydrazone of salicylaldehyde (**2c**) and the pyrrole-2-carboxaldehyde (see ESI† for the details).

resulted in a variety of readily accessible BOPBY, BOBHY, and BOSPY dyes, offering unique optical behaviors.[17] Although these dyes also share stereogenic-at-boron characteristics similar to those of BASHY, no chiroptical investigation has been conducted yet.

Building on our previous interest in developing chiral dyes,[15b] in this communication, we describe the development of structurally diverse novel fluorophores (**1a–h**) through a tri-component reactions of commercially available salicylaldehyde derivatives (**2a–c**) and arylboronic acids (**3a–c**) with readily accessible 2-formylpyrrole hydrazones (**4a–d**) in a single step (Scheme 1). The stereogenic boron center in these compounds provides access to unique chiral-at-boron fluorophores (**1a–h**) through enantiomeric resolution on chiral HPLC column.

This assembly system is designed with two key features in mind: ready availability of starting materials and (2) facile diversification potential through the use of substrates with diverse substitution patterns. Capitalizing on these advantages, we successfully synthesized compound **1a** in a reasonable yield of 32% under optimized reaction condition (see ESI†). The reaction involved refluxing an equimolar mixture of 4-(diethylamino)salicylaldehyde (**2a**), phenylboronic acid (**3a**), and the hydrazone of pyrrole-2-carbaldehyde (**4a**) in acetonitrile for 24 hours (Scheme 1). The chemical structure of **1a** was unequivocally confirmed by NMR spectroscopy, high-resolution mass spectrometry (HRMS), and single-crystal X-ray diffraction analysis (see ESI† and Fig. 3). Next, to explore the reaction's versatility, we performed the reaction with structural variations at each component: the pyrrole (**1a–d**), the salicyl-aldehyde/-ketone (**1a**, **1e**, and **1h**), and the arylboronic acid (**1a**, **1f**, and **1g**) units. The herein developed one-step, tri-assembly MCRs served as an enabling platform for efficient synthesis of fused tetracyclic boron-chelates **1a–h**, despite the moderate yields (12–32%, Scheme 1), for which conventional synthetic approaches failed to give any trace of product (Scheme S5, ESI†).

The model dye **1a** exhibited very low solvent-dependent absorbance and fluorescence—solvatochromism (Fig. S40, ESI†). It absorbs maximally at around 450 nm and emit at around 530, displaying large Stokes shifts ($\Delta\lambda \sim 3000$ cm^{-1}).[18]

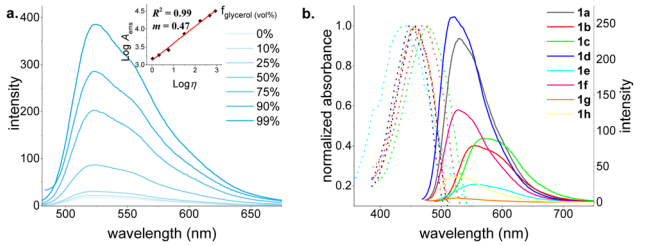

Fig. 2 (a) Fluorescence emission spectra of **1a** in glycerol–ethanol mixtures with varying glycerol fractions [$f_{glycerol}$ (vol%): 0–99%] at 25 °C. Integrated area ratio of $f_{glycerol\,(0\%)}/f_{glycerol\,(99\%)} \sim 1/21$. (b) Normalized UV-vis absorption and fluorescence emission spectra of the BOSPYR dyes (**1a–h**, 2 μM) in DMSO.

Following the work by Hao and coworkers[17c] on the aggregation-induced emission (AIE) properties of structurally similar BOSPY dyes, we investigated the emission properties of our BOSPYR dyes, in water–DMSO mixtures (Fig. S41, ESI†). The fluorescence intensity exhibits negligible enhancement, gradually increasing up to 50% water fraction, followed by a sharp decrease at higher water fractions, likely due to aggregation or precipitation (Fig. S41, ESI†). To understand the dimmed fluorescence emissions of **1a** in organic solvents, we recorded emission spectra in glycerol–ethanol mixtures with varying glycerol fractions (Fig. 2a). The fluorescence intensity increased by 21-fold when switching from pure ethanol to pure glycerol. The enhanced fluorescence observed in viscous glycerol medium suggests non-radiative vibrational relaxations as a key quenching mechanism for the dye **1a**, making it a promising tool for studying biological processes associated with increased extracellular viscosity.[19,20]

To understand the influence of structural variations on optical properties, we recorded absorption and fluorescence emission spectra for all BOSPYR dyes (**1a–h**) in DMSO (Fig. 2b and Table S1, ESI†). All dyes exhibit large Stokes shifts (2633–4930 cm^{-1}) and weak emission (Φ_{fl}: 1.5–9.1%)[21] with fluorescence lifetimes ranging from 0.47 to 2.00 ns, all characterized by a monoexponential fit. Alkyl substitution on the pyrrole unit (**1a** to **1c**; entries 1–3, Table S1, ESI†) induces a bathochromic shift (530–573 nm). A more pronounced red-shift is observed for ethyl substitution at the pyrrole's 3-position (**1c**) compared to dimethylation (**1b**). Electrostatic potential surface calculations for compounds **1b** and **1c** (Fig. S51, ESI†) indicate

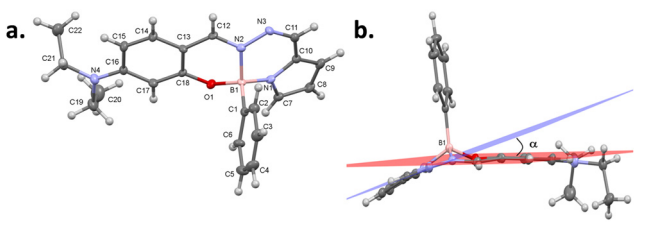

Fig. 3 (a) X-ray molecular structure of **1a** with the atom-numbering scheme. Displacement ellipsoids are drawn at the 40% probability level. (b) Dihedral angle between chelating mean planes defined by atoms N1–C10–C11–N3 and C13–C18–O1–C12; α = 17.2°.

Open Access Article. Published on 05 N'wendzamhala 2024. Downloaded on 2026-05-24 15:17:00.
This article is licensed under a Creative Commons Attribution-NonCommercial 3.0 Unported Licence.

that alkyl groups with mild electron-donating character decrease the energy required for reorganizing the delocalized π-network by increasing electron density on the pyrrole ring. This lowers the energy gap between ground and excited states, resulting in the observed bathochromic shift. Compared to **1a**, compound **1d** exhibits a small but noticeable blue shift in both absorption and emission maxima, accompanied by a 3-fold enhancement in quantum yield. Interestingly, removing the $-NEt_2$ group on the salicylaldehyde unit (**1a** *vs.* **1e**) leads to divergence of the absorption and emission maxima. While the absorption maximum of **1e** exhibits a 20 nm blue shift, its emission maximum undergoes a 27 nm red shift, resulting in the largest Stokes shift of 4930 cm^{-1} (see Table S1, ESI†). This modification comes at the expense of a five-fold decrease in molar absorptivity and reduced chemical stability (Fig. S45, ESI†). The absence of the strong electron-donating $-NEt_2$ group is believed to destabilize compound **1e**, leading to lower electron density and reduced π-electron delocalization. Consequently, this results in a smaller transition dipole moment and hence a lower molar absorptivity compared to the others. Although thermally somewhat stable, it readily degrades upon exposure to mild acids and bases, and even undergoes solvolysis by DMSO (Fig. S46 and S47, ESI†). This is consistent with its reduced aromaticity revealed by DFT computation (*vide infra*). To explore the influence of the electronic nature of the pendant aryl unit, we synthesized dyes **1f** and **1g** simply by varying arylboronic acid substrate. As expected, the absorption and emission maxima of these dyes were nearly identical to those of the model dye **1a**, consistent with electronic decoupling between the aryl unit and the chromophore. The minimal influence of electronic effects on the absorption and emission properties of the aryl unit introduced *via* the arylboronic acid module makes this position particularly attractive for a broad range of labeling applications.

To gain detailed structural insight, single crystals of **1a** suitable for X-ray diffraction analysis were obtained by slow evaporation from methanol (Fig. 3 and Fig. S53, ESI†). The structure confirms the exact conformation of **1a**, which crystallizes as a racemate in the centrosymmetric triclinic $P\bar{1}$ space group. Both enantiomers occupy the asymmetric unit with opposite configurations at the boron center. Complexation around the boron atom leads to a four-fused ring system. The B–N chelate bonds within each molecule range from 1.515 to 1.588 Å. Additionally, B–O coordination bonds are observed with B1–O1 (1.482(3) Å) and B2–O2 (1.468(3) Å). The boron atoms exhibit slightly distorted tetrahedral geometries, displaced by 0.569 Å (B1) and 0.560 Å (B2) from the planes defined by the tri-coordinated O1/N1/N2 and O2/N5/N6 atoms, respectively. The dihedral angle between the mean planes of N1–C10–C11–N3 and C13–C18–O1–C12 is 17.2 degrees (Fig. 3).

The presence of a stereogenic boron atom in all BOSPYR dyes (**1a–h**) prompted us to investigate the chiroptical properties of enantiomerically pure **1a**. (±)-**1a** was resolved *via* high-performance liquid chromatography (HPLC) using an analytical chiral column (Chiralcel® OD-H) under isocratic conditions (eluant: *n*-hexanes : 2-propanol; 98 : 2). Gratifyingly, chiral HPLC separations were well achieved for the remaining racemic dyes (**1b–h**) as well (see ESI† for methods). The presence of two well-separated peaks with comparable integrated areas in the chiral HPLC chromatogram confirms the successful separation of enantiomers (Fig. S9, ESI†). The isolated enantiomers exhibited significant optical activity ($[\alpha]_D^{25}$ −2054.8° *vs.* +2082.2°, $CHCl_3$), uncommon for small, point-chiral organic molecules.[13–15] This mirror-image relationship in their specific rotations (almost equal but opposite in sign) is another strong indication of their enantiomeric nature. To assess the configurational stability of dye **1a**, toluene solutions of (−)-**1a** were refluxed under open-air atmosphere for 1 hour. Gratifyingly, no epimerization was observed with chiral HPLC analysis (see Section S5.2 in ESI†), indicating high configurational stability. Compound (±)-**1a** demonstrated high stability towards light, acids (except acids like TFA), and bases (Fig. S43 and S44, ESI†).

The ECD spectra of (+)-**1a** and (−)-**1a** confirmed their relative configurations (Fig. S10, ESI†). The large specific rotations and distinct Cotton effects ($|g_{abs}| \sim 1.9 \times 10^{-3}$, λ_{ext} 457 nm) suggest that the twisted planarity of the molecule, revealed by the X-ray structure, should contribute significantly to its pronounced chiroptical activity and inherent chirality.

To understand the excited state properties, computational studies were performed using DFT and TD-DFT methods. B3LYP-D3 provided the best agreement with experimental UV-vis spectra, accurately reproducing dihedral angle (17.3° *vs.* 17.2°) and λ_{abs} values (Fig. S49, ESI†). Vibrational frequency calculations and excited state geometry optimizations confirmed the thermal and photostability of most dyes. An exception was observed in molecule **1e**, where the first triplet excited state exhibited ring deformations due to reduced aromaticity. The structure of **1e** was also characterized by its low dipole moment and polarizability in the absence of the $-NEt_2$ group, which explains the observed emission trends (Table S3, ESI†). The calculated UV-vis spectra for the first 30 singlet excited states agreed well with experimental data, including the red-shifted peaks observed in **1b** and **1c** (Fig. S49, ESI†). Analysis of natural transition orbitals for the first singlet excited state (S_1) of **1a–1h** (Fig. 4 and Table S4, Fig. S51, ESI†) revealed that the main absorption involves delocalized π-electrons across the chromophore, extending to the diethyl amine group upon excitation. This $S_0 \rightarrow S_1$ excitation exhibits a locally excited (LE) state character, as evidenced by the redistribution of electron density within the conjugated ring structure, which accounts for the weak fluorescence (Fig. 4 and Fig. S51, S52, ESI†). This phenomenon is further corroborated by ground-state and excited-state atomic charge distribution analyses (Fig. S54, ESI†).[22] Interestingly, theoretical calculations could not reproduce the experimental fluorescence spectra. Key computed parameters, including a singlet–triplet energy gap (ΔE_{ST}) of 0.75 eV, a reorganization energy ($\lambda_{S_1/T_1-S_1/S_1}$) of 0.2 eV, and spin–orbit coupling matrix elements (SOCME) for S_1/T_1 of 9.54×10^{-5} eV for **1a**, suggest a low reverse intersystem crossing rate (k_{RISC}) of 3.13×10^{-11}. These findings rule out the possibility of these dyes acting as thermally activated delayed fluorescence (TADF) emitters. Additionally, the optimized geometry of the first excited state revealed a rotation of the B–Ph group, which may contribute to the observed enhancement of emission in viscous media (Fig. S48, ESI†).

 This journal is © The Royal Society of Chemistry 2025

Open Access Article. Published on 05 N'wendzamhala 2024. Downloaded on 2026-05-24 15:17:00.
This article is licensed under a Creative Commons Attribution-NonCommercial 3.0 Unported Licence.

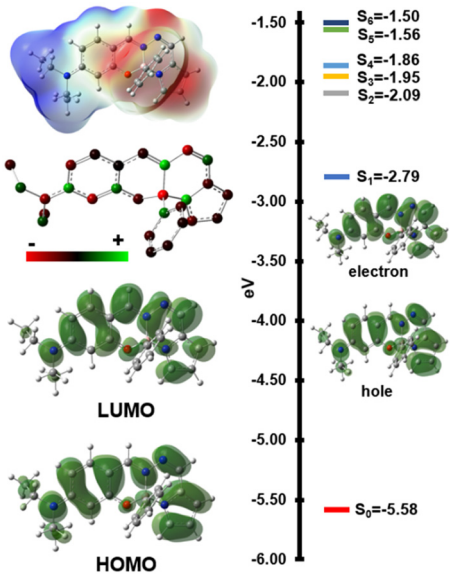

Fig. 4 ESP, charge distribution, HOMO and LUMO surfaces, singlet energy levels and natural transition orbitals of $S_0 \rightarrow S_1$ transition for **1a**.

The HOMO–LUMO energy gap decreased from 2.8 eV to 2.3 eV upon excited state geometry optimization, highlighting the influence of geometry relaxation on the emission spectra (*e.g.* large $\Delta\lambda$) and supporting the solvent-independent emissions observed experimentally (Fig. S40, ESI†). This relaxation also led to a good correlation between the electrochemical bandgap calculated through differential pulse voltammetry (DPV) experiments and the computed optical bandgap (2.27 eV *vs.* 2.30 eV, Fig. S47 and Table S2, ESI†).

In conclusion, this work presents a powerful approach for the synthesis of diverse stereogenic-at-boron BOSPYR fluorochromes through a straightforward one-step MCR. This method offers several advantages: it utilizes readily available starting materials, enables creation of fluorophores with an asymmetry at the boron atom, and yields visible light-absorbing dyes with large Stokes shifts and weak fluorescence that can be significantly enhanced in viscous media, making them promising viscosity imaging probes. Additionally, the inherent chirality of these fluorophores, arising from the bent conformation of the chromophore, evidenced by the large specific rotations and distinct Cotton effects of **1a**, opens exciting possibilities for their development as chiroptical tools. The high configurational stability of B-stereocenter in these chelates further highlight them as reliable chiral fluorochromes. The combination of efficient synthesis, tunable properties, and inherent chirality positions these dyes as versatile, promising building blocks for advanced functional materials.

Data availability

Additional data supporting this article have been included as part of the ESI.†

Conflicts of interest

There are no conflicts to declare.

Notes and references

1 (*a*) J. R. Lakowicz, *Principles of fluorescence spectroscopy*, Springer Science + Business Media, New York, 3rd edn, 2006; (*b*) H. Zollinger, *Color chemistry: syntheses, properties, and applications of organic dyes and pigments*, Wiley-VCH, 2003.
2 (*a*) D. Frath, J. Massue, G. Ulrich and R. Ziessel, *Angew. Chem., Int. Ed.*, 2014, **53**, 2290; (*b*) H. Kim, A. Burghart, M. B. Welch, J. Reibenspies and K. Burgess, *Chem. Commun.*, 1999, 1889; (*c*) W. Zhao and E. M. Carreira, *Angew. Chem., Int. Ed.*, 2005, **44**, 1677; (*d*) X. Li, G. Zhang and Q. Song, *Chem. Commun.*, 2023, **59**, 3812.
3 (*a*) A. Loudet and K. Burgess, *Chem. Rev.*, 2007, **107**, 4891; (*b*) G. Ulrich, R. Ziessel and A. Harriman, *Angew. Chem., Int. Ed.*, 2008, **47**, 1184; (*c*) N. Boëns, V. Leen and W. Dehaen, *Chem. Soc. Rev.*, 2012, **41**, 1130.
4 N. Boens, B. Verbelen and W. Dehaen, *Eur. J. Org. Chem.*, 2015, 6577.
5 (*a*) L. Levi and T. J. J. Müller, *Chem. Soc. Rev.*, 2016, **45**, 2825; (*b*) F. de Moliner, N. Kielland, R. Lavilla and M. Vendrell, *Angew. Chem., Int. Ed.*, 2017, **56**, 3758; (*c*) L. Brandner and T. J. J. Müller, *Front. Chem.*, 2023, **11**, 1124209; (*d*) A. Vázquez-Romero, N. Kielland, M. J. Arévalo, S. Preciado, R. J. Mellanby, Y. Feng, R. Lavilla and M. Vendrell, *J. Am. Chem. Soc.*, 2013, **135**, 16018.
6 F. M. F. Santos and J. N. Rosa, *et al.*, *Chem. – Eur. J.*, 2016, **22**, 1631.
7 P. M. S. D. Cal and F. Sieglitz, *et al.*, *Chem. Commun.*, 2017, **53**, 368.
8 M. M. Alcaide and F. M. F. Santos, *et al.*, *J. Org. Chem.*, 2017, **82**, 7151.
9 V. G. Jiménez and F. M. F. Santos, *et al.*, *J. Org. Chem.*, 2018, **83**, 14057.
10 F. M. F. Santos and Z. Domínguez, *et al.*, *ChemPhotoChem*, 2018, **2**, 1038.
11 B. Zhang, S. Wang, J. Tan and X. Zhang, *Dyes Pigm.*, 2018, **155**, 186.
12 M. J. S. A. Silva and Y. Zhang, *et al.*, *Bioconjugate Chem.*, 2023, **34**, 2337.
13 H. Lu and J. Mack, *et al.*, *Coord. Chem. Rev.*, 2016, **318**, 1.
14 (*a*) T. E. Wood and N. D. Dalgleish, *et al.*, *J. Am. Chem. Soc.*, 2005, **127**, 5740; (*b*) E. M. Sánchez-Carnerero and F. Moreno, *et al.*, *Chem. Commun.*, 2013, **49**, 11641; (*c*) S. Kolemen, Y. Cakmak, Z. Kostereli and E. U. Akkaya, *Org. Lett.*, 2014, **16**, 660; (*d*) E. M. Sánchez-Carnerero and F. Moreno, *et al.*, *J. Am. Chem. Soc.*, 2014, **136**, 3346; (*e*) R. I. Lerrick and T. P. L. Winstanley, *et al.*, *Chem. Commun.*, 2014, **50**, 4714; (*f*) T. Bruhn and G. Pescitelli, *et al.*, *Angew. Chem., Int. Ed.*, 2014, **53**, 14592; (*g*) Y. Wu, S. Wang, Z. Li, Z. Shen and H. Lu, *J. Mater. Chem. C*, 2016, **4**, 4668; (*h*) Y. Gobo, M. Yamamura, T. Nakamura and T. Nabeshima, *Org. Lett.*, 2016, **18**, 2719; (*i*) M. Saikawa, T. Nakamura, J. Uchida, M. Yamamura and T. Nabeshima, *Chem. Commun.*, 2016, **52**, 10727; (*j*) R. B. Alnoman and S. Rihn, *et al.*, *Chem. – Eur. J.*, 2016, **22**, 93; (*k*) R. Clarke and K. L. Ho, *et al.*, *ChemPhotoChem*, 2017, **1**, 513; (*l*) J. Jiménez and L. Cerdán, *et al.*, *J. Phys. Chem. C*, 2017, **121**, 5287; (*m*) M. Toyoda, Y. Imai and T. Mori, *J. Phys. Chem. Lett.*, 2017, **8**, 42; (*n*) Y. Gobo, R. Matsuoka, Y. Chiba, T. Nakamura and T. Nabeshima, *Tetrahedron Lett.*, 2018, **59**, 4149; (*o*) C. Maeda, K. Nagahata, T. Shirakawa and T. Ema, *Angew. Chem., Int. Ed.*, 2020, **59**, 7813; (*p*) H. Sakai and Y. Suzuki, *et al.*, *J. Mater. Chem. C*, 2023, **11**, 2889.
15 (*a*) A. Hafele, C. Zedde, P. Retailleau, G. Ulrich and R. Ziessel, *Org. Lett.*, 2010, **12**, 1672; (*b*) M. Işık, E. Dündar, E. Şahin and C. Tanyeli, *Chem. Commun.*, 2022, **58**, 7188; (*c*) B. Zu, Y. Guo, L.-Q. Ren, Y. Li and C. He, *Nat. Synth.*, 2023, **2**, 564; (*d*) R. G. Clarke and J. Weatherston, *et al.*, *ChemPhotoChem*, 2023, **7**, e202200194; (*e*) C. Ray and E. Avellanal-Zaballa, *et al.*, *Org. Chem. Front.*, 2023, **10**, 5834.
16 (*a*) N. Algoazy and J. G. Knight, *et al.*, *Chem. – Eur. J.*, 2021, **27**, 5246; (*b*) B. Zu, Y. Guo and C. He, *J. Am. Chem. Soc.*, 2021, **143**, 16302; (*c*) Y. Sun and C. Yu, *et al.*, *Chem. Commun.*, 2023, **59**, 13986; (*d*) G. Zhang and Z. Zhang, *et al.*, *Nat. Commun.*, 2022, **13**, 2624.
17 (*a*) N. Chen and W. Zhang, *et al.*, *Org. Lett.*, 2017, **19**, 2026; (*b*) J. Wang and X. Fang, *et al.*, *Org. Lett.*, 2021, **23**, 4796; (*c*) H. Wang and X. Guo, *et al.*, *Dyes Pigm.*, 2023, **210**, 111013.
18 A. Dhara and T. Sadhukhan, *et al.*, *J. Am. Chem. Soc.*, 2020, **28**, 12167.
19 K. Bera and A. Kiepas, *et al.*, *Nature*, 2022, **611**, 365.
20 M. Paez-Perez and M. K. Kuimova, *Angew. Chem., Int. Ed.*, 2024, **63**, e202311233.
21 Relative fluorescence quantum yields were calculated using quinine sulphate as the reference (Φ_{fl} = 0.60 in 0.5 M H_2SO_4). See: A. M. Brouwer, *Pure Appl. Chem.*, 2011, **83**, 2213.
22 F. Weinhold and J. E. Carpenter, in *The Structure of Small Molecules and Ions*, ed. R. Naaman and Z. Vager, Plenum, 1988, pp. 227–236, DOI: 10.1007/978-1-4684-7424-4.